

We B04

Analysis of Viscous Crossflow in Polymer Flooding

M. H. Alshawaf* (Imperial College London/ Saudi Aramco), S. Krevor (Imperial College London) & A. Muggerridge (Imperial College London)

SUMMARY

Polymer flooding improves oil recovery by improving flood front conformance compared with waterflooding as well as, in some cases, extracting more oil from lower permeability zones in the reservoir by viscous cross-flow. However viscous cross-flow of water from the low permeability zone may also adversely affect the polymer flood by causing the polymer slug to be diluted and possibly to lose its integrity. The extent to which viscous cross-flow improves or reduces recovery depends upon the permeability contrast between the low and high permeability zones, the viscosity ratios of the fluids (oil, water and polymer solution) and the geometry of the layers. This paper uses inspectional analysis to derive the minimum set of 6 dimensionless numbers that can be used to characterise a polymer flood in a two layered model. A series of finely gridded numerical simulations are then performed to determine the contribution of viscous crossflow to oil recovery from secondary and tertiary polymer flooding in this system. We show that viscous cross-flow will only make a positive impact on oil recovery from secondary polymer flooding when the viscosity ratio values of oil to polymer solution is less than 1 and permeability ratio between the layers is less than 50. Furthermore, we show that there is an inverse relationship between the permeability ratio between layers and the amount of degradation the polymer slug experiences due to viscous crossflow in the high permeability layer. As the permeability contrast between layers increases, the slug degradation decreases. Also, the results show that the desired positive impact from viscous crossflow is higher in secondary polymer floods when compared to tertiary polymer floods. Finally, the results can be used to make initial estimates of the contribution of both viscous cross-flow and mobility control in polymer flooding applications without the need to perform extensive and time consuming numerical simulations.

Introduction

When a production strategy is being designed for an oil reservoir, reservoir engineers prioritise flood front conformance. Achieving flood front conformance brings benefits in stratified reservoirs with contrasting permeabilities. Having a near uniform flood front means that the oil in the reservoir is being recovered efficiently both vertically and areally. Moreover, uniform flood fronts helps delaying early and unnecessary water breakthrough that results in increasing handling costs from layers with high permeabilities (Sorbie, 1991). Although research showed that even in unfavourable mobility ratios crossflow does improve overall recoveries in communicating stratified reservoirs compared to non-communicating reservoirs (Zapata and Lake, 1981, Ahmed *et al*, 1988), however, reservoir engineers can still design special flood projects to improve recoveries further and gain economic benefits beyond what ordinary waterflood projects offer (Sorbie, 1991).

One of the options used frequently in the industry is to implement polymer floods as an Enhanced Oil Recovery (EOR) technique to improve recoveries. Traditionally, polymer floods are implemented as a mobility control method to improve oil recoveries by lowering mobility ratio to values close to unity or lower through increasing the viscosity of the injected water (Pye, 1964., Sandiford, 1964., Sorbie, 1991., Lake, 1989). The increase in viscosity is achieved by adding water-soluble polymers with experimentally determined concentrations to obtain optimum flood viscosities that will improve recoveries and project economics.

An added benefit of using polymer floods, if designed properly, is inducing additional viscous crossflows between adjacent communicating layers. Consequently, fronts in different layers with different permeabilities are closer compared to the same situation under waterfloods, or in other words, achieving an improved flood front conformance. Viscous crossflow occurs due to the difference in the vertical pressure gradients caused by the different positions each polymer front/slug occupy in their respective layers. (Sorbie, 1991, Sorbie and Seright, 1992, Seright, 2016). For example, in a simple two-layered model with constant pressure boundaries, the slug in the high permeability layer will be advancing faster than the normally smaller and slower slug in the lower permeable layer. In an ideal situation under favourable mobility ratio polymer floods, the pressure gradient behind the slug in the high permeability layer will cause a viscous crossflow of water and polymer solution to the lower permeability layer. This action coupled with lower pressure gradients ahead of the polymer slug in the higher permeability layer causes oil to flow from the lower permeability layer to the higher permeability layer to balance the crossflow at the back of the slug as well as extracting more oil from the low permeability layer compared to no crossflow cases (Clifford and Sorbie, 1985; Sorbie, 1991, Wright *et al*, 1987). This type of crossflow leads to closer flood fronts amongst the different layers of a reservoir.

The magnitudes of crossflow that improve recovery in stratified reservoirs depend on the mobility ratios between oil, polymer solution and water and the permeability contrast between adjacent layers. Moreover, with crossflow occurring between adjacent layers, a reduction in polymer slug size is observed at the back of the slug travelling through the higher permeability layer that if not accounted for may destroy the slug (Sorbie, 1991). The magnitude of dilution of polymer slug size is also controlled by the viscosities of the displacing and displaced fluids as well as the contrast between the adjacent layers. As the permeability contrast and mobility ratio between polymer solution and oil increase the amount slug size dilution decreases.

The effects of viscous crossflow have been investigated experimentally and numerically by many researchers in the past decades (Sorbie *et al*, 1990; Clifford and Sorbie, 1985; Sorbie and Walker, 1988; Seright, 2016; Shotton *et al*, 2016). Their research focused mainly on how viscous crossflow occurs and how it qualitatively impacts the position of the flood fronts in the low and high permeability layers. These research tended to focus on the case when high water cuts have been reached with limited number of cases. Some researchers have investigated viscous crossflow in the presence of other displacing forces such as capillary and gravity effects and determined which

displacing force prevails in controlling flood fronts at different combinations of flow rates, fluid densities and IFT (Cinar *et al.*, 2006; Alhamdan *et al.*, 2011, Debbabi *et al.*, 2016).

In addition, some researchers have examined crossflow in the context of gel placement and how to minimise it so that the gel slug injected in the high permeability layer can be placed as far as possible in the reservoir to efficiently divert chase water into the low permeability layers (Sorbie and Seright, 1992). Gel placement, unlike polymer floods, require a mobility ratio close to unity between a gel slug and chase water to minimise the crossflow of gel material in to the low permeability layer that will cause irreversible formation damage. On the other hand, one of the main goals of polymer flooding is maximise beneficial viscous crossflow through injecting a highly viscous slug in the stratified reservoir.

This paper, unlike previous studies, analyses the cumulative oil recoveries of numerous polymer and water floods scenarios with communicating and non-communicating layers to develop a quantitative relationship between the amount of viscous crossflow and reservoir and fluid properties. The paper sheds light on several important aspects of polymer flooding. Firstly, we derive through inspectional analysis the 6 dimensionless numbers necessary to describe a polymer flood in a simple two-layered model with constant pressure boundaries. Secondly, we use ECLIPSE 100 to run finely gridded simulation scenarios to determine the contribution of crossflow on a layer level and to determine the implications this has on the total field production and cumulative recovery. Thirdly, we take a look at how starting polymer floods earlier in the life of the field gives better recoveries and hence better project economics. Fourthly, we show the trends of slug size dilution in the high permeability layer in both secondary and tertiary polymer flood modes. Finally, we show the optimum slug size required to maximise the viscous crossflow values to improve recoveries.

Methodology

Inspectional Analysis

It is very important that a thorough set of laboratory coreflood experiments precede any pilot or field wide implementation of a new production strategy such as polymer flooding. Equally important is understanding the results of these coreflooding experiments and grasping the assumptions surrounding the experiment because certain displacing forces that might act in laboratory corefloods might not be present on a reservoir scale and vice versa (Sorbie 1991). Therefore, an incorrect interpretation of the results may lead to wrong scaled up values of, for example, polymer concentrations which ultimately leads to either the failure to achieve reservoir engineering goals, cost overruns or both (Sorbie, 1991). In addition, it is important to derive the necessary scaling parameters for polymer flooding in stratified reservoirs because they will help reservoir engineers determine the dominant flow regimes (viscous crossflow or mobility control) in polymer flooding without running time consuming and complex reservoir scale simulations.

We used inspectional analysis to drive the 6 necessary dimensionless groups that describe polymer floods in stratified reservoirs under constant pressure boundaries. Inspectional analysis uses the partial differential equations that describe the physical laws of the system in question as well as the initial and boundary conditions. (Shook *et al.* 1992).

To minimize the complexity of the problem, the following assumptions were made:

- The polymer solution is a Newtonian fluid.
- Physical dispersion is minimised.
- No adsorption in the model that leads to loss of viscosification of the solution or any pore plugging by the polymer molecules that might lead to Inaccessible Pore Volume (IPV).

These assumptions were also implemented in the numerical part of the study for consistency. We have followed the methodology outlined by Shook *et al* (1992) to drive the dimensionless groups. The six dimensionless groups are as follows:

Table 1 List of dimensionless numbers produced through inspectional analysis.

Dimensionless Groups Description	Dimensionless Group
Aspect ratio for isotropic systems	$\frac{L}{H}$
Dimensionless permeability ratio	$\frac{k_b}{k_{eff}}$
Thickness ratio	$\frac{h}{H}$
Layer permeability ratio	$\frac{k_a}{k_b}$
Dimensionless flood viscosity ratio	$\frac{\mu_w}{(\mu_{p,max} - \mu_w)}$
Modified mobility ratio	$\frac{k_{rw}^0 \mu_0}{(k_{ro}^0)(\mu_{p,max} - \mu_w)}$

L , H and h are the system's length, total thickness and the thickness of the high permeability layer. k_a , k_b , k_{eff} are the permeabilities of layers a , b and the effective permeability in the direction of flow. μ_w , μ_o , and $\mu_{p,max}$ represent the viscosities of water, oil and the maximum polymer solution viscosity corresponding to the concentration at the injector. Finally, k_{rw}^0 and k_{ro}^0 are the end point relative permeabilities for water and oil respectively.

The dimensionless flood viscosity number and the modified mobility number are new and never been derived before. The other numbers have been produced previously to address other multiphase flow problems, Table 1 (Shook *et al*, 1992). Using the difference between the polymer solution and water viscosities as a scaling factor in the model reduces the number of dimensionless groups. This technique eliminated the need to have two different mobility ratios for the water/oil and polymer solution/oil systems. The modified mobility ratio now incorporates all of the viscosity values into one dimensionless number.

To test the validity of the dimensionless groups, three different simulation scenarios at different scale sizes were run, Table 2. For each scale size, the 6 dimensionless groups were kept the same, Table 3, and the results of the dimensionless cumulative oil production and water cut for each case were compared to each other. Figure 1 shows the results of the 3 cases with excellent agreement validating the 6 dimensionless groups produced from inspectional analysis. The group will be used later on to plot and interpret the crossflow results under different rock and fluid properties.

Table 2 The mobile oil pore volume for the different scale sizes used to test the validity of the dimensionless groups produced through inspectional analysis.

Scale Size	Mobile Oil Pore Volume (MOPV)
Lab	2.4E-05 m ³
Large Slab	1.2E+00 m ³
Reservoir	1.2E+06 m ³

Table 3 Table of the dimensionless group numbers and the values that were used in the numerical simulator for the different scale sizes to test the validity of the inspectional analysis approach that produced the dimensionless groups.

Dimensionless Group Name	Value
Aspect Ratio (L/H)	2
Thickness Ratio (h/H)	0.5
Layer Permeability Ratio (k_a/k_b)	3.5
Dimensionless Permeability Ratio (k_b/k_{eff})	0.44
Dimensionless Flood Viscosity ratio ($\mu_w/\mu_p-\mu_w$)	0.05
Modified Mobility Ratio	0.53

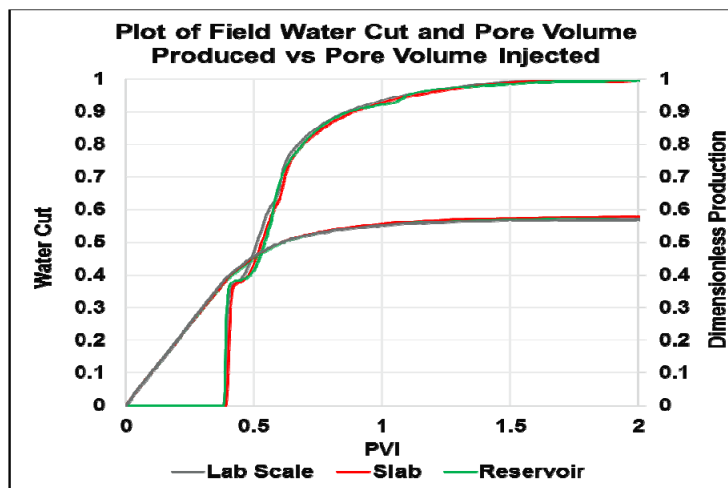


Figure 1 Simulation result showing the water cut and dimensionless cumulative production vs. pore volume injected. The results show that when the 6 dimensionless numbers that were produced through inspectional analysis are kept the same, the results of water cut and dimensionless cumulative production will be the same for all a cases irrespective of scale size.

The Viscous Crossflow Mechanism

A two-dimensional, two-layered simulation model was created to study the mechanism of viscous crossflow, a phenomena that occurs in the flooding of vertically stratified reservoirs, in particular, we focus on viscous crossflow due to the injection of polymer slugs. In a vertically stratified reservoir with contrasting layer permeabilities and under constant pressure boundary conditions, injecting a slug of polymer solution will result in the slugs in each layer being at different positions after some period of injection. The constant pressure boundary condition used in the simulation runs was an appropriate choice because it replicates the conditions that the slugs experience deep in the reservoir where the pressure at the boundaries are assumed to be constant.

If we inject a polymer slug under constant pressure boundaries in a simple two layered model, Figure 2, where the bottom layer has a permeability value approximately several times larger than that of the permeability of the top layer, the slug in the high permeability layer will advance faster as seen in the example of a model with non-communicating layers in Figure 3. Therefore, the pressure profiles with distance in each layer will be different as can be seen in Figure 4.

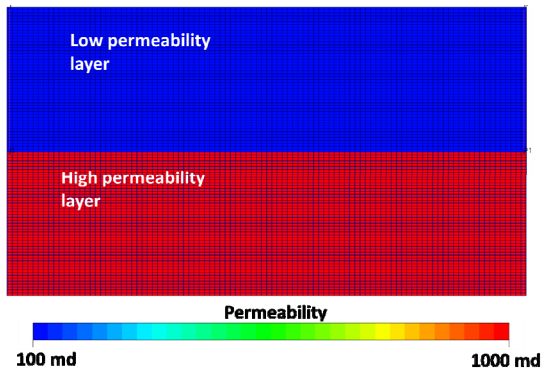


Figure 2 Permeability of the model in the x direction

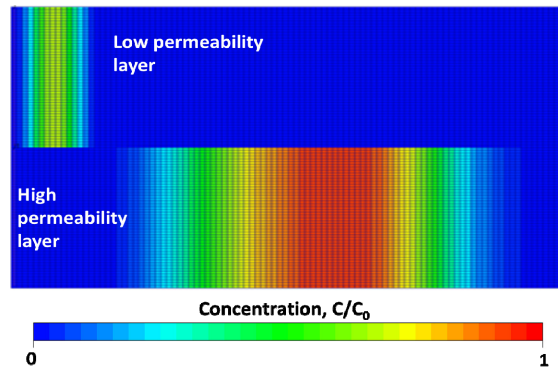


Figure 3 shows the different positions of the ideal, non-adsorbent polymer slugs in the non-communicating layers advancing at different rates

Continuing on with the viscous crossflow illustration example, Figure 4 shows that the pressure at the leading edge of the slug in the high permeability layer is lower than the pressure in the low permeability layer, while the opposite is the case at the back of the slug where the pressure of the high permeability layer is higher than the pressure in the lower permeability layer. No crossflow takes place in this case because of the no communication assumption that we have initially put in place. If the communication between the layers is re-established, then the system will tend to equilibrate, and for this to happen a crossflow of fluids must occur at the front and rear of the polymer slug residing in the high permeability layer (Sorbie, 1991).

As mentioned previously, the pressure at the slug front advancing in the high permeability layer is lower than the pressure in the corresponding position in the low permeability layer. This situation will induce viscous crossflow of oil at the leading edge of the slug from the low to the high permeability layer. Therefore, the high permeability layer will produce more oil than its original oil in place by the time all of the movable oil is produced. Moreover, to balance the aforementioned oil crossflow at the slug front, water and some polymer solution crossflows from the high to the low permeability layer due to the higher pressure at the rear of the advancing slug in the high permeability layer. Therefore, by the time all of the movable oil has been produced from the model, the low permeability layer would have produced less oil than its original oil in place. In addition, the crossflow of water and polymer solution at the back of the slug in the high permeability layer does not only cause crossflow of oil to the high permeability layer at the front of the slug, it also extracts and accelerates the production of oil in the low permeability layer (Sorbie and Walker, 1988). Because of this combination of processes, a better flood front conformance is achieved. Figure 5 shows an example of a polymer concentration map for a model with communicating layers and viscous crossflow on going around the ideal polymer slug in the high permeability layer.

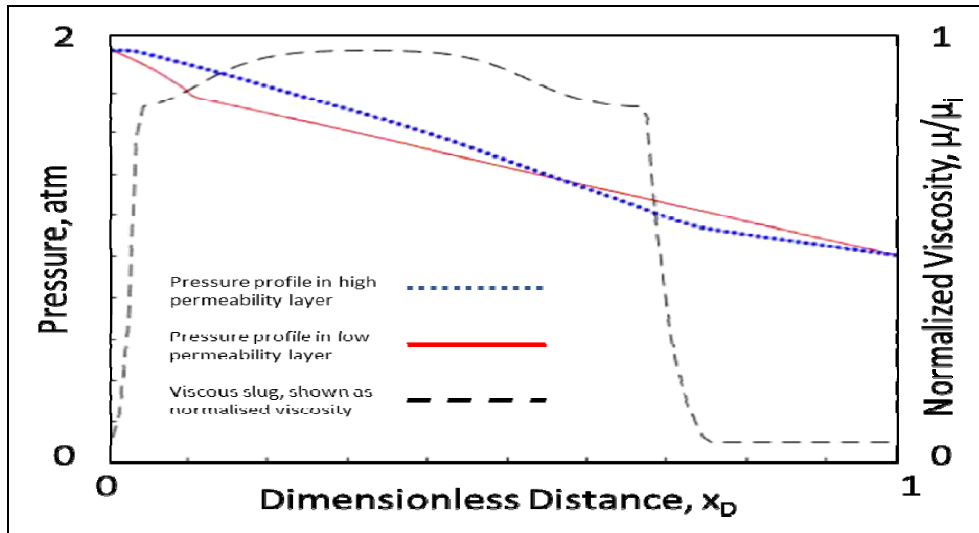


Figure 4 Pressure profiles in each layer and the position of the polymer slug in the high permeability layer.

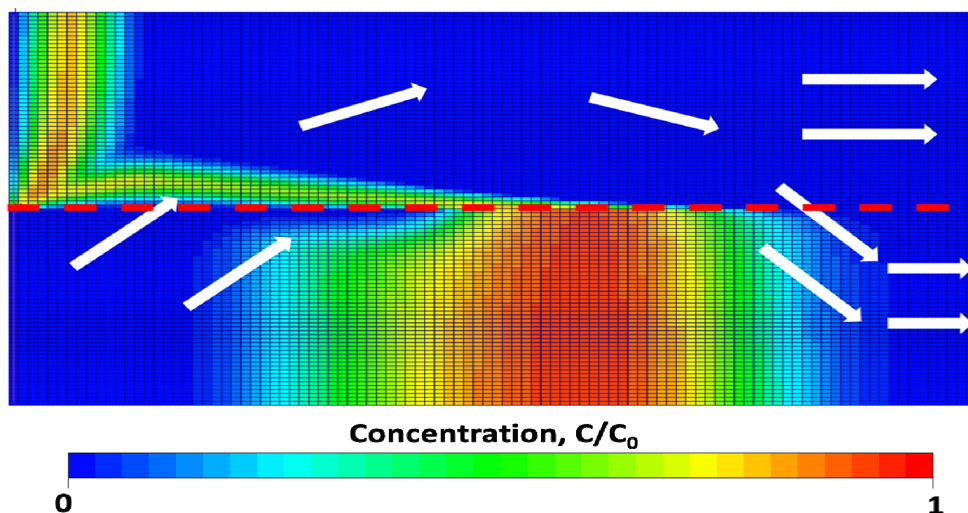


Figure 5 An example showing the polymer slugs advancing in each layer at different rates in a fully communicating layers model with crossflow clearly evident.

Simulation Model Setup, Assumptions and Methodology:

The simulation model is a 2D laboratory scale model of the following dimensions 20cm×10cm×0.5cm. For the crossflow study, the model consists of two layers. The top layer is designated to be the low permeability layer, while the bottom layer is designated to be the high permeability layer. Polymer flooding usually targets heavy oil reservoirs characterized by densities close to that of water. Therefore in the model oil and water were assigned density values of 0.95 g/cc and 1 g/cc respectively. Capillary pressure in the model was eliminated by setting it to zero. The polymer slug used in this study is assumed to be an ideal viscous slug. To ensure that we have an idea slug in the simulation runs, the following assumptions have been implemented in the model:

- No polymer adsorption onto the rock and hence there will be no retardation of the slug front.
- IPV value of 0% so that all pores are accessible to the polymer molecules and therefore no acceleration of the slug front.

- A “square” like slug is maintained throughout the model as shown by the black dashed line in Figure 4. This was achieved by modifying the polymer concentration vs. polymer solution viscosity table to have the viscosity maintained at very low concentration.
- The viscous slug is a Newtonian fluid.
- A Todd-Longstaff mixing parameter value of 0.95

A summary of the simulation model, rock and fluid properties of the base case used for this study can be found in Table 4.

Table 4 Summary of properties of base case model.

Porosity (ϕ)	40%	
High Permeability Layer (k_a)	1000	md
Low Permeability Layer (k_b)	100	md
Layer Permeability Ratio (k_a/k_b)	10	
Layers Thickness Ratio (h_a/H)	0.5	
Oil Viscosity (μ_o)	10	cp
Water Viscosity (μ_w)	1	cp
Polymer Solution Viscosity (μ_p)	20	cp
Oil to Polymer Viscosity Ratio (μ_o / μ_p)	0.5	
Cell Length	20	cm
Cell Width	10	cm
Cell Depth	0.5	cm
Cells x Direction	100	
Cells y Direction	100	
Cells z Direction	1	
Residual Oil Saturation (S_{or})	0.2	
Connate Water Saturation (S_{wc})	0.2	
Oil Corey Exponent (n_o)	1.5	
Water Corey Exponent (n_w)	5	
End Point Oil Relative Permeability (k_{ro}^0)	1	
End Point Water Relative Permeability (k_{rw}^0)	1	
Capillary Pressure (P_c)	0	atm
Oil Density (ρ_o)	0.95	g/cc
Water Density (ρ_w)	1	g/cc
Adsorption	0	g/cc
Inaccessible Pore Volume (IPV)	0	%
Initial Model Pressure (P_0)	2	atm
Injection BHP (P_{in})	2	atm
Production BHP (P_{out})	1	atm
K_v Multiplier in Communicating Layers	1	
K_v Multiplier in Non-communicating Layer	0	
Todd-Longstaff Mixing Parameter (ω)	0.95	

As mentioned previously, the purpose of this study is to investigate the parameters that impact crossflow in a simple two-layered system under polymer flooding with constant pressure boundaries. In this study the layer ratio of permeabilities in the two layers is investigated alongside the modified mobility ratio derived from our inspectional analysis of the physics of polymer flooding. For ease of reference we would like to note that throughout this paper the term secondary floods refers to polymer floods starting at the beginning of production of the system while the term tertiary refers to polymer floods that start when the system’s water cut reaches a value of 90%.

Layer permeability ratios of {1, 2.5, 3.5, 5, 10, 25, 37, and 50} and modified mobility ratios of {0.53, 0.81, 1.1, 4.3, and 10} were simulated for models with communicating layers and then repeated again with no communication or flow in the y-direction between the two layers to eliminate viscous crossflow. Benchmark waterflood runs were also run for the previously mentioned layer permeability ratios for scenarios with and without communication between the layers. Comparing the communicating and non-communicating models in each simulation scenario allow us to isolate the additional recoveries resulting from the viscous crossflow effect from the recovery that results from the favourable mobility ratio that the polymer flooding also provides. The crossflow and mobility control results were reported at 1 and 3 PVI for secondary and tertiary polymer floods respectively.

This paper also investigated how the polymer slug size is affected by dilution through viscous crossflow. The dilution was quantified by comparing the mass of polymer injected in the high permeability layer with the mass of polymer produced as the trailing edge of the polymer slug reaches the producer in the high permeability layer.

The final part of the paper also investigates how slug size impacts the amount of additional recovery in polymer floods as rock and fluid properties are varied for the field level. In this investigation, we looked at the cases where the layer permeability ratio is 3.5 and modified mobility ratios of 0.53 and 10. Polymer slug sizes investigated were {0, 0.1, 0.25, 0.4, 0.5, 0.75 and 1} pore volumes.

All cases are run under constant pressure boundary conditions, which means that the cases cannot be compared with each other using real time because the Pore Volumes (PV) injected are different at each time in each case. Therefore, the cumulative production versus time curves rescaled to cumulative production versus PV injected. The viscous crossflow sign convention is the following, if the values are positive it indicates that crossflow has accelerated the production by the computed pore volumes when compared with a case with no communication and whilst negative crossflow values indicate a deceleration of production. In this paper, the focus will be on the viscous crossflow from the perspective of the total system and will be referred to as the field level. Therefore, the comparison will be between the production and injection data for communicating and non-communicating models considering the whole field.

Results and Discussion

Running the different layer permeability and modified mobility ratios mentioned previously resulted in a total of 80 simulation cases (40 cases with communicating layers and 40 cases for non-communicating layers). The results of the 80 secondary polymer flooding cases produced 40 crossflow values at different combination of layer permeability and modified mobility ratio. Figure 6 combines all these results in a contour plot after 1 PVI for the field level. It can be seen that at favourable modified mobility ratios (below or equal to 1.11) and a moderate permeability contrast between the communicating layers, there is a significant viscous crossflow of oil. In addition, viscous crossflow improves recoveries in almost all cases including ordinary waterfloods in reservoirs with communicating layers as shown by the green curve in Figure 6. The results in the figure also show that the highest viscous crossflow contribution to overall recovery is observed to be between the layer permeability ratios of 3.5 and 5 after injecting a total of 1PV of polymer solution and chase water (approximately 11.3% MOPV). Finally, as expected there is no crossflow for the homogeneous system (permeability contrast of 1).

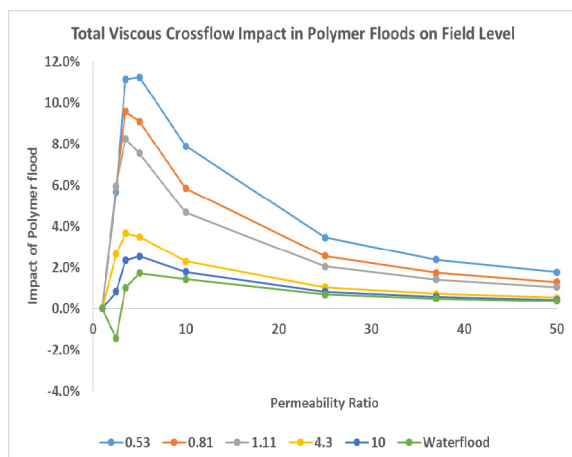


Figure 6 A summary plot of the total impact of viscous crossflow in polymer floods on a field level after 1 PVI. The green curve is a summary of the ordinary waterflood runs. Each curve is a constant modified mobility ratio value. Layer permeability ratio is on the x-axis and percentage of crossflow contribution on the y-axis.

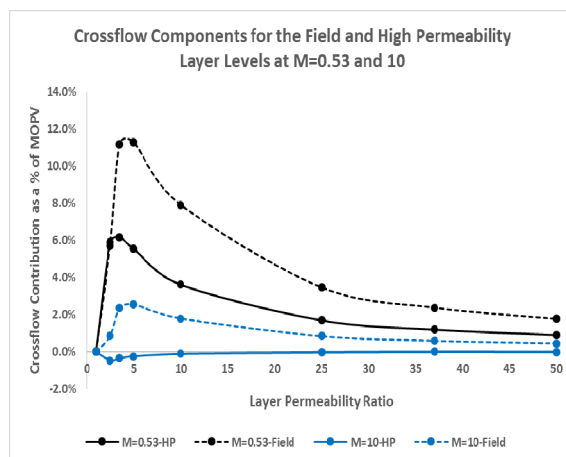


Figure 7 A plot showing the crossflow components for the field and high permeability layer levels at $M=0.53$ and 10 after 1 PVI. Layer permeability ratio is on the x-axis and percentage of crossflow contribution on the y-axis.

The magnitude by which crossflow improves the overall recovery in both layers depends on the mobility ratio. All modified mobility ratio cases examined in this study improve recovery by two processes. As mentioned previously, when a fraction of a pore volume has been injected into the system, the slugs in each layer will be in different positions due to the different permeabilities each layer has. Figure 5 presented earlier in this paper illustrates the two processes that occur simultaneously as both slugs advance in the system.

The first process occurs when polymer solution and chase water crossflow from the back of the polymer slug in the high permeability layer to displace more oil out of the low permeability layer as opposed to situations where crossflow is prohibited. The second process is the balancing oil crossflow effect that takes place at the front of the polymer slug due to the crossflow of water and polymer solution at the back of the slug. Figure 7 shows a graph of the viscous crossflow components of the field and high permeability layer levels for two different modified mobility ratios. The field level crossflow component at the favourable mobility ratio of 0.53 is more positive than the high permeability layer crossflow component which indicates that there is also a contribution that came from the low permeability layer by virtue of the cross-flowed polymer solution and chase water at the back of the slug in the high permeability layer. The additional amount of oil that was extracted from the low permeability layer due to viscous crossflow is much higher than the amount of oil that has cross-flowed from the low to the high permeability layer, therefore, resulting in a positive net gain of oil in the low permeability layer at the modified mobility ratio of 0.53.

The same conclusion can be drawn from the unfavourable modified mobility ratio of 10 although, the amount of oil extracted from the low permeability layer in this case is less than that obtained from the favourable mobility ratio case for all layer permeability ratios. When the modified mobility ratio is higher than 1.11 the only process that contributes to the improvement of recovery is the fluids crossflowing from the high to the low permeability layer displacing more oil from the low permeable layer.

Now that we have quantified the values of viscous crossflow, the next step is to determine how much crossflow contributes to the overall improvement in oil recover from polymer flooding after 1 PVI injection using a polymer slug followed by chase water. To be able to determine the contribution of viscous crossflow in polymer floods, first the contribution due to mobility improvement must be

determined. This is calculated by subtracting the cumulative recovery curves from particular non-communicating water flooding case from the corresponding non-communicating polymer flooding case.

Figure 8 shows a summary of the percentage of incremental oil produced due to mobility control. The figure shows that, expected, incremental oil is maximised at the lowest modified mobility ratio values. Once the contribution of improving mobility ratios is determined the, contribution of viscous crossflow to the overall contribution of polymer flooding in the high permeability layer is calculated. Figure 9 shows the contribution of viscous crossflow to the incremental oil produced in secondary polymer floods. This value was calculated by taking the viscous crossflow contribution and dividing it by the total contribution due to polymer flood. The figure indicates that viscous crossflow dominates the displacement mechanism at modest layer permeability ratios and high unfavourable modified mobility ratios. As the viscosity of the injected slug increases and the permeability contrast increases, mobility control dominates the displacement mechanism.

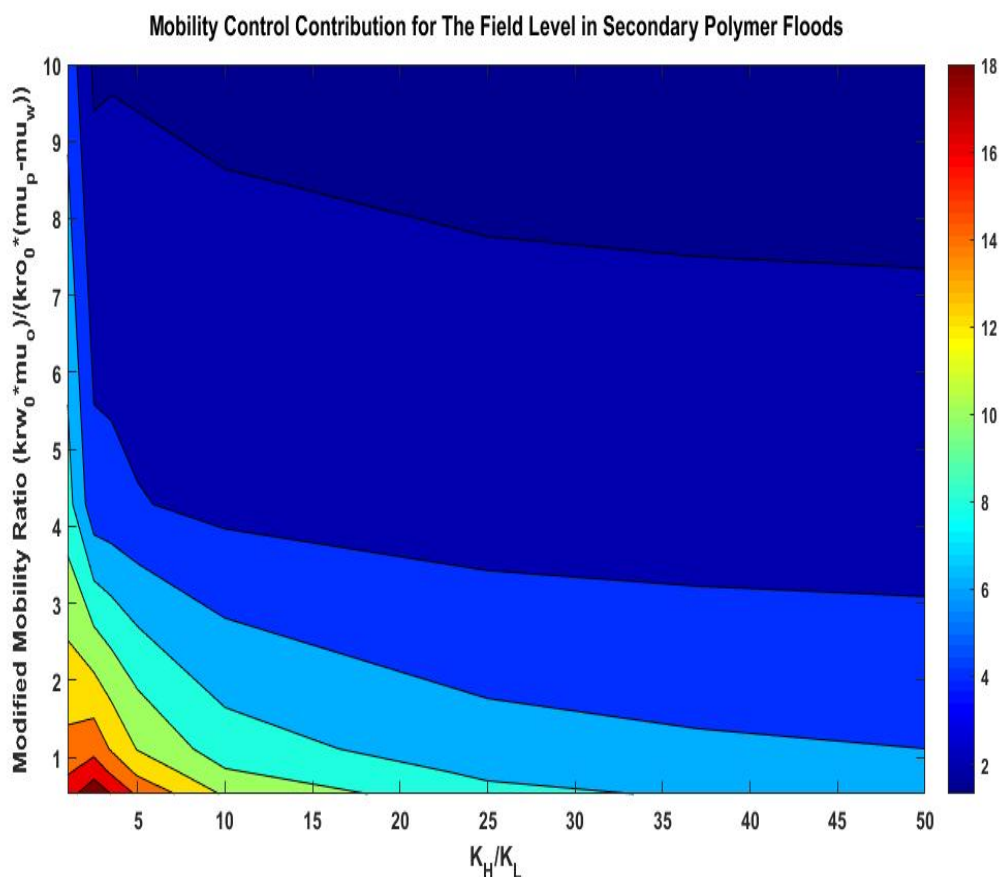


Figure 8 Percentage contribution of mobility control in secondary polymer floods at $PVI=1$. Layer permeability ratio is on the x-axis. Modified mobility ratio on the y-axis.

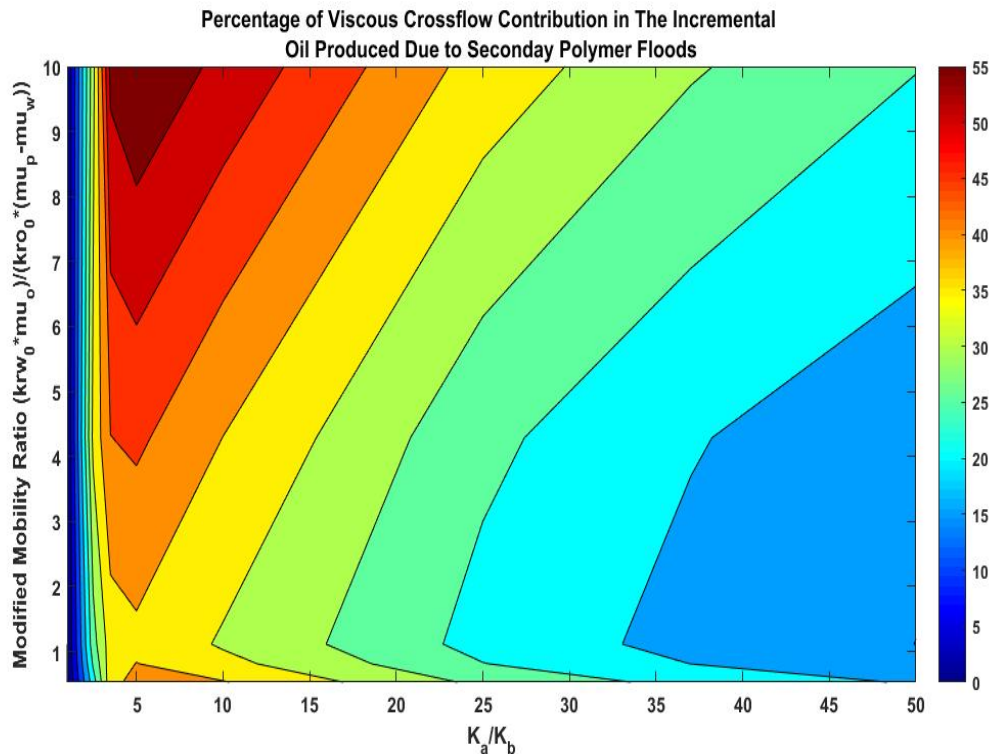


Figure 9 Contour maps showing the percentage of the contribution made by viscous crossflow in the incremental oil produced by secondary polymer floods at PVI= 1. Permeability ratio is on the x-axis. Modified mobility ratio on the y-axis. The value was calculated by adding the viscous crossflow and the mobility control components to obtain the total contribution of polymer floods. Then the viscous crossflow was divided by the entire contribution to obtain the percentage.

In terms of flood front conformance, viscous crossflow improved the flood front conformance as can be seen in the oil saturation maps at different fractions of PVI in Figures 10 to 13. Figures 10 and 11 show a comparison between two polymer floods at 0.25 and 0.5 PVI of polymer solution and chase water respectively for the case of 3.5 layer permeability ratio and 0.53 for the modified mobility ratio. The “No Crossflow” model is at the top and the “Crossflow” model is at the bottom in both figures. The white dashed line shows the positions of the flood fronts in the model with communicating layers for comparison with the flood front position in the non-communicating layers. The conclusion here is that flood front in the high permeability layer advances faster in the model with no vertical communication than the flood front in the model with the communicating layers. In addition, the flood front in the low permeability layer in the non-communicating layer advances slowly than in the model with communicating layer. The distance between the fronts in the communicating and non-communicating models grows larger as more fluids are injected. Therefore, the model with communicating layers will have better recoveries than in the cases with non-communicating layers.

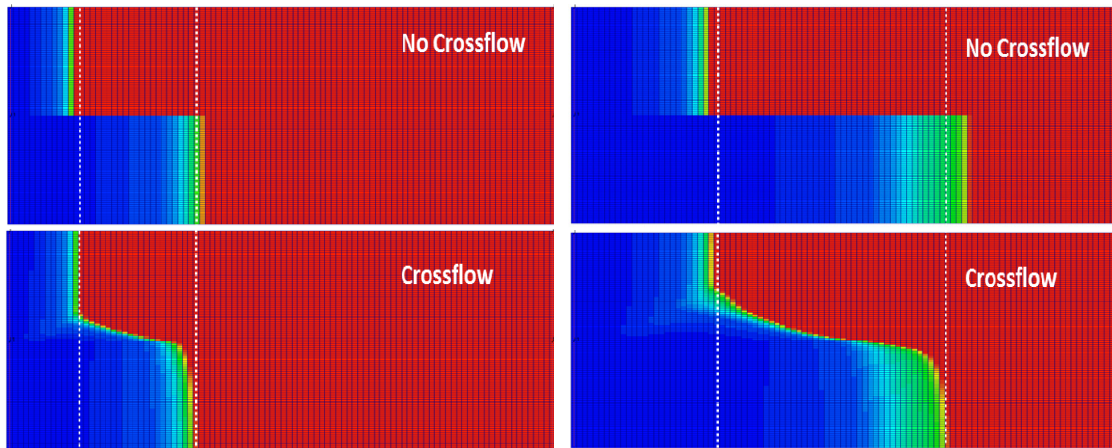
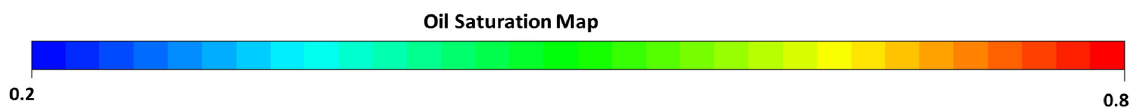


Figure 10 A comparison between a non-communicating and communicating polymer flood models with a layer permeability ratio of 3.5 and a mobility ratio of 0.53 at 0.25 PV of injection. The white dashed line show the flood front positions in both layer for the communicating mode.

Figure 11 A comparison between a non-communicating and communicating polymer flood models with a layer permeability ratio of 3.5 and a mobility ratio of 0.53 at 0.5 PV of injection. The white dashed line show the flood front positions in both layer for the communicating mode.



Figures 12 and 13 show a comparison between a waterflood case and a polymer flood case after injecting 0.25 and 0.5 PV of polymer solution and chase water. Both models have communicating layers to allow for crossflow. The improvement due to the polymer flood is clearly visible. Viscous crossflow improves the flood conformance by ensuring that the flood front in the low and high permeability layer are closer compared to the water flood case. In addition, polymer flood provided better sweep of the oil behind the flood fronts in both layers as compared with the waterflood with an unfavourable mobility ratio. Therefore, we see a significant improvement in oil production profiles when a slug of polymer with the right characteristics is injected into this stratified reservoir. The improvement is characterised by a considerable delay of water breakthrough leading to more oil produced up front and hence better project economics.

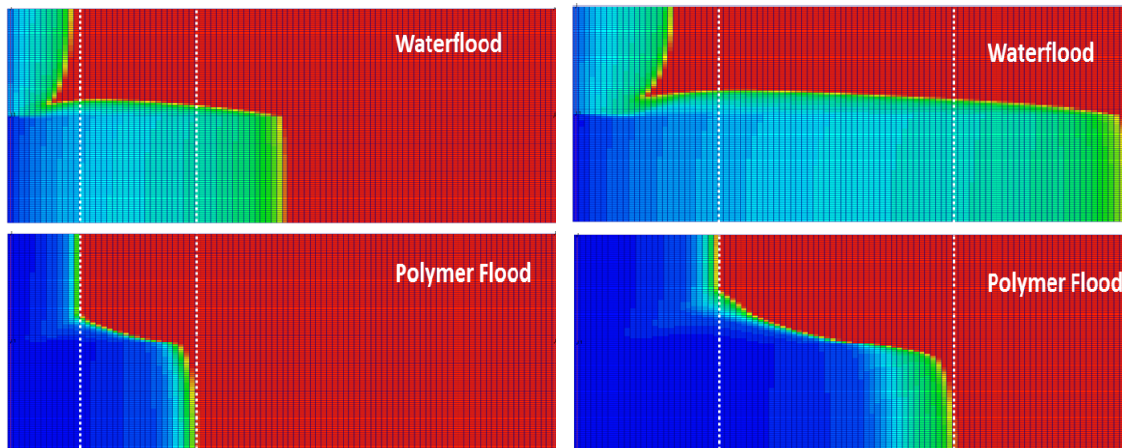


Figure 12 A comparison between a water flood and a polymer flood models with communicating layers with a layer permeability ratio of 3.5 at 0.25 PV of injection. The white dashed line show the flood front positions in both layer for the communicating mode.

Figure 13 A comparison between a water flood and a polymer flood models with communicating layers with a layer permeability ratio of 3.5 at 0.5 PV of injection. The white dashed line show the flood front positions in both layer for the communicating mode.

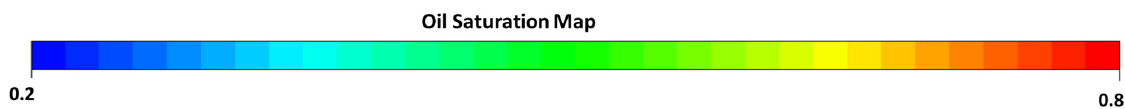


Figure 14 shows the total crossflow contribution from both layers in tertiary polymer floods. From the figure, the crossflow peaks at a permeability ratio of 10 with a contribution of 7% MOPV compared to 5 and 11.3% MOPV for layer permeability ratio and contribution respectively in secondary polymer floods. That is expected since the remaining oil in tertiary polymer floods is less than in secondary polymer floods. The contribution of mobility control to the overall recover is shown in Figure 15, the additional oil recovered drops between permeability ratios of 1 and 3.5 and then peaks at a ratio of 5 where it then decreases again as the layer permeability ratio increases. The reason for this trend is because the 90% water cut trigger values occur after more pore volumes of water have been injected for the cases of 2.5 and 3.5. Thus, until the injection of the polymer slug starts the oil will be produced by only ordinary waterflood. By the time the slug starts, there is less oil in the model to be contacted by the slug and consequently affects the amount of oil that is produced by mobility control.

Figure 16 shows the total incremental oil recovered from a tertiary polymer flood on a contour map. A negative overall polymer flood contribution is observed at unfavourable modified mobility ratios and modest layer permeability ratios. That is because viscous crossflow hinders the production in the field and negates any gains made by mobility control at moderate layer permeability ratios and high unfavourable mobility ratios. One might argue that the results calculated from each individual case that was run as a tertiary polymer flood for this study should not be compared to each other because the polymer slugs started at different average remaining field oil saturation due to the variation of layer permeability ratios. In practice when polymer floods are considered or implemented it will be initiated based on aggregate production numbers for the whole field. Therefore, the analysis presented here mimics the activities and considerations made in the actual field.

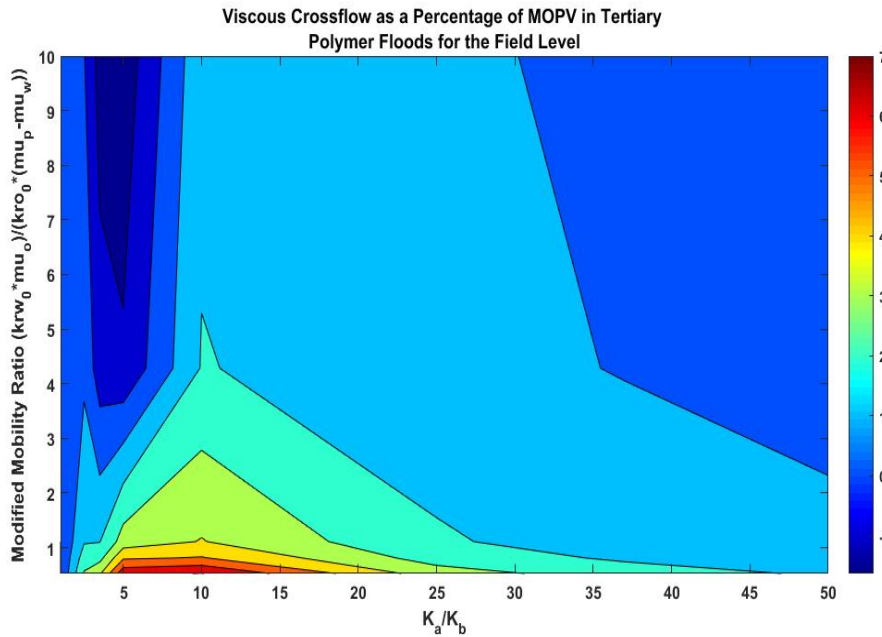


Figure 14 Contour map showing viscous crossflow as a percentage of MOPV in polymer floods for the field level at PVI=3. Layer permeability ratio is on the x-axis and modified mobility ratio on the y-axis.

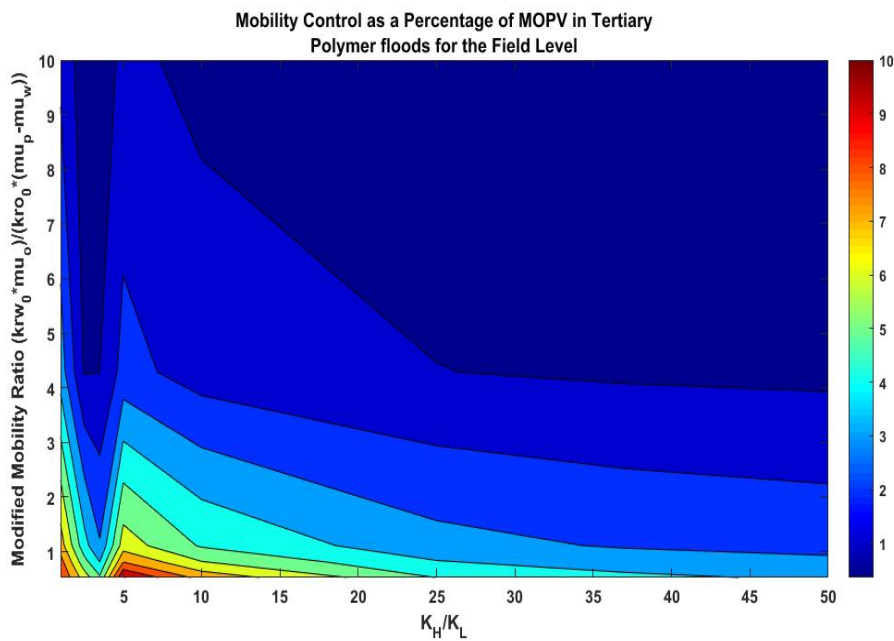


Figure 15 Contour map showing mobility control as a percentage of MOPV in polymer floods for the field level at PVI=3. Layer permeability ratio is on the x-axis and modified mobility ratio on the y-axis.

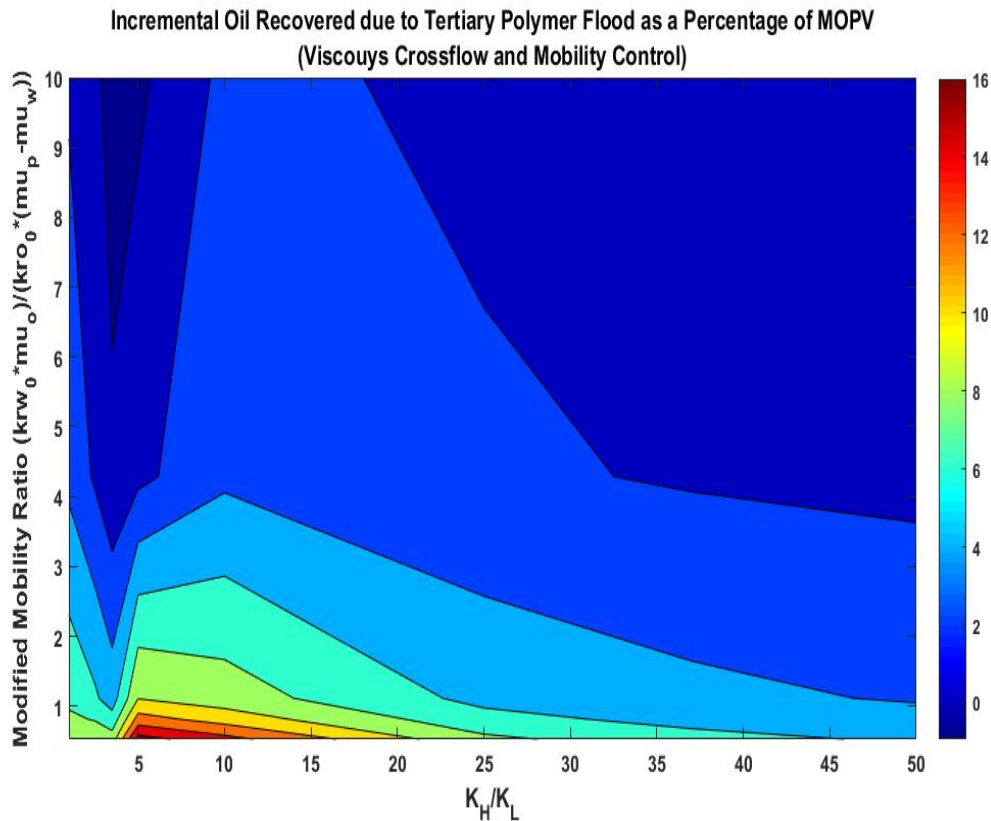


Figure 16 Percentage of incremental oil recovered at $PVI=3$ due to tertiary polymer flood for the field level. The contour map was constructed by adding the crossflow and mobility control components. Layer permeability ratio is on the x-axis and modified mobility ratio on the y-axis.

Figure 17 illustrates of the crossflow in a tertiary simulation run after injecting 0.82 PV of the following sequence of fluids: lead water then polymer slug and finally followed by chase water. The top plot is an oil saturation map for a model with non-communicating layers, while the bottom plot is for a model with a communicating layers. The results are for the runs with a layer permeability ratio of 5 and a modified mobility ratio of 0.53. In the non-communicating layers model, the injection of a polymer slug after 90% water cut has been reached creates an oil bank ahead of the slug, which is marked by an increase in the oil saturation as indicated in the non-communicating model in Figure 17. On the other hand, in the communicating layers model we can clearly see the viscous crossflow in action crossflowing from the low to the high permeability layer in addition to the oil bank that is being developed as the slug moves forward. A visual example for the secondary polymer floods cases was not possible because the oil that is crossflowing from the low permeability layer to the higher permeability crossflows into virgin oil sections ahead of the polymer slug.

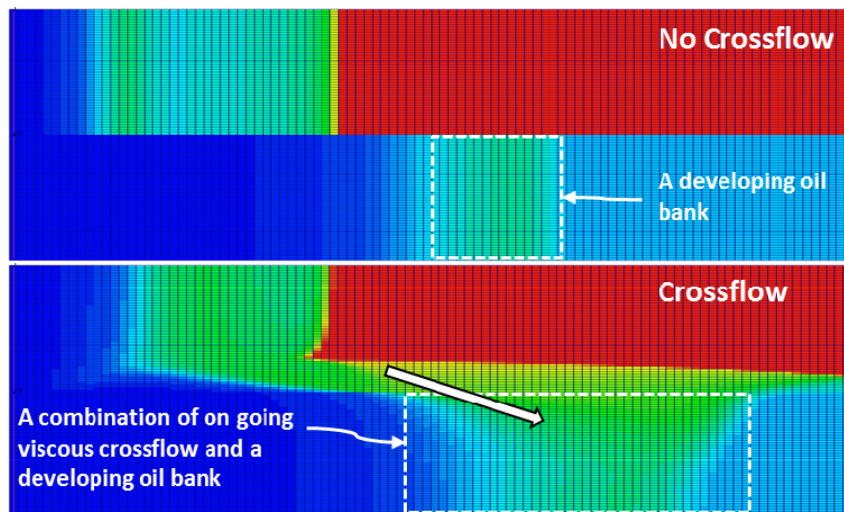
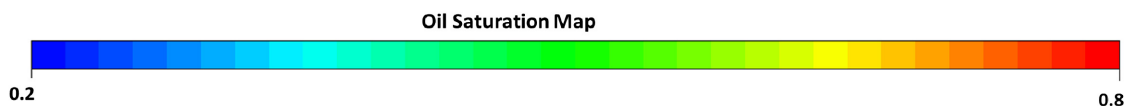


Figure 17 An oil saturation maps for non-communicating and communicating layers models in tertiary polymer floods. The runs are for a layer permeability ratio of 5 and a modified mobility ratio of 0.53. There is a clear visual of viscous crossflow in the case on communicating layers in addition to the expected oil bank that leads the polymer slug as the slug moves forward.



Crossflow is an excellent way of maximising recovery through means of viscosity modification of water, however, it can also hinder the success of a polymer flooding project because of the dilution of the polymer slug by the crossflow of chase water. As stated previously, polymer slugs are injected in reservoirs to improve microscopic displacement by reducing the mobility ratio through increasing the viscosity of water. Polymer slugs are also injected to improve the vertical sweep efficiency by viscous crossflow due to the differential pressure gradients between the layers at the back and the leading edge of the polymer slug. Polymer solution and chase water both crossflow from the high to the low permeability layer at the back of the slug. Therefore, with time the entire slug could crossflow to the low permeability layer and displace the oil (Sorbie, 1991).

However, if this happens before the slug in the higher permeability layer contacts all the oil in its layer then the benefits could be limited. Therefore, a proper slug size must be determined precisely to ensure that full benefit is achieved from polymer floods. In our analysis, the percentage of slug size dilution by viscous crossflow was determined by dividing the amount of polymer mass produced at the time the trailing edge of the polymer slug reaches the producer in the high permeability layer to the total mass of polymer injected in the high permeability layer. Figure 18 shows the impact of dilution by viscous crossflow on the slug size as the modified mobility ratio and layer permeability ratios in secondary polymer floods are varied. Positive percentage values indicate a dilution of the slug at that particular permeability and modified mobility ratios. The figure shows that as both layer permeability ratio and modified mobility ratio increase, slug dilution decreases, an inverse relationship. In the runs performed for this paper, the largest dilution of the slug occurred at a modified mobility ratio of 0.53 and permeability ratio between 2.5 and 3.5, which corresponds accordingly to where maximum crossflow of oil occurs.

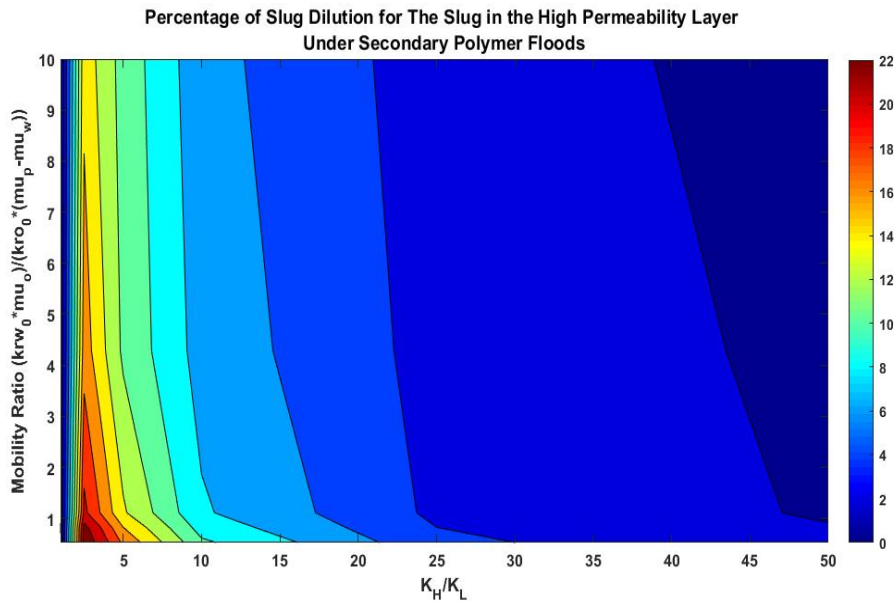


Figure 18 A contour map showing the values of polymer slug reduction as the layer permeability (x-axis) and modified mobility ratio (y-axis) vary in secondary polymer floods at PVI=1. The results shown here are for the high permeability layer.

The results in tertiary polymer floods echo those of secondary polymer floods. Slug size dilution in tertiary polymer floods is minimised as the permeability and mobility ratios increase as can be seen in Figure 19. Also, slug dilution in tertiary polymer floods are less than their counterparts in secondary polymer floods due to reduction in viscous crossflow.

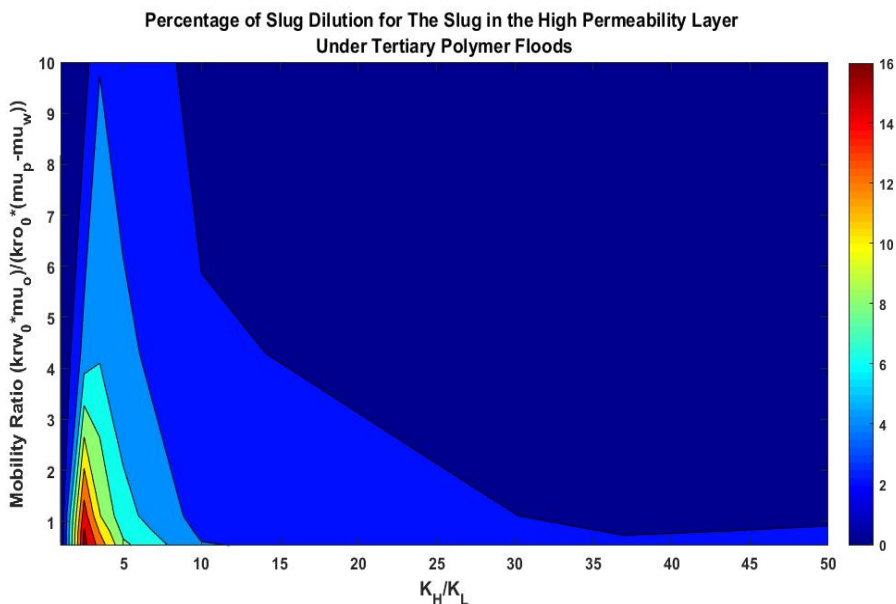


Figure 19 A contour map showing the values of polymer slug reduction as the layer permeability (x-axis) and modified mobility ratio (y-axis) vary in tertiary polymer floods at PVI=3. The results shown here are for the high permeability layer.

The final part of the paper focuses on the impact of the size of the polymer slug that is injected on the magnitude of viscous crossflow. Results from the system’s entire production, Figure 20, show interesting trends. The figure shows a breakdown of the total crossflow showing the crossflow in the high and low permeability layers for modified mobility ratios of 0.53 and 10 respectively. The crossflow for the field level shows that the maximum crossflow occurs for a slug size of 0.1 PV followed by a decrease in the amount of viscous crossflow as the slug size increases to 1 PV. To

explain this observation, we mentioned earlier that in certain cases the additional oil recovered due to viscous crossflow is due to two processes. The polymer solution and chase water that crossflows from the high to low permeability layer at the back of the slug causes an acceleration of oil production from the low permeability layer in addition to oil cross flowing to the high permeability layer ahead of the slug. Thus, as the slug size increases beyond the 0.1 PV mark we see a reduction in the amount of oil extracted from the low permeability layer which results in the net crossflow effect in the low permeability changing from positive to negative after 0.5 PVI mark. This means that beyond a slug size of 0.5 PVI the additional oil extracted from the low permeability layer is not enough to offset the crossflow of oil from the low to the high permeability layer at the front of the slug resulting in a net negative viscous crossflow value for the low permeability layer. However, when the crossflow component is added to the mobility control component, Figure 21, the peak additional oil is achieved around 0.4 PV. We observe a high diminishing marginal return as the slug size increases beyond the 0.4 PV marker which might make the economics unfavourable beyond that point.

The optimum value of 0.4 PVI calculated here is for an ideal slug that does not experience adsorption or loss of viscosity during its progression from injector to producer. Adding those variables, for example, might lead to different optimum slug size, but, in essence the total losses the polymer slug might experience in the reservoir should not lead to a net slug size less than 0.4 to obtain maximum benefits from polymer floods.

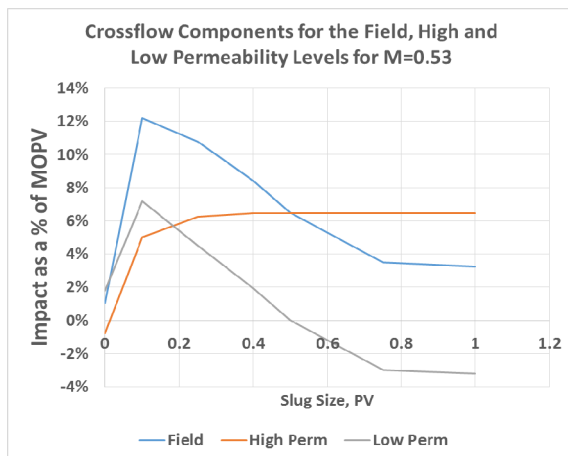


Figure 20 A plot showing the crossflow components for secondary polymer floods of field, high and low permeability layer levels for $M=0.53$ vs. polymer slug size.

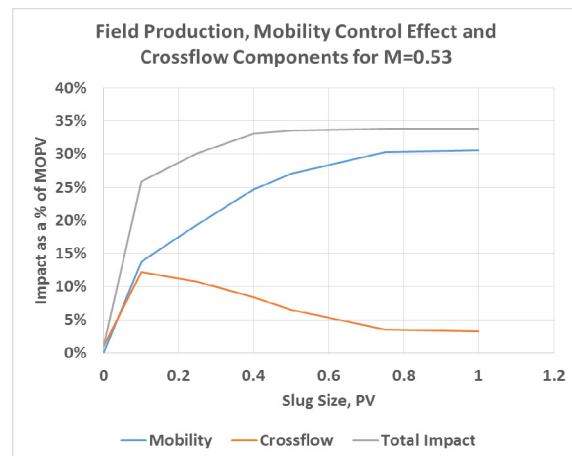


Figure 21 Plot showing a breakdown of total secondary polymer flooding impact to a viscous crossflow and mobility control components at $M=0.53$ vs. slug size.

When the mobility ratio is unfavourable such as the example of a modified mobility ratio of 10, we see similar trends to that for a favourable mobility ratio. However, the crossflow mechanism in unfavourable modified mobility ratio cases is different. Before the polymer slug breaks through from the high permeability layer, a large viscous crossflow of oil happens over the entire length of the model from the high to the low permeability layer because the pressure in of the higher permeability layer is higher than that of the low permeability layer. When the slug breaks through in the high permeability layer the pressure profiles in both layers reverse such that the pressure in the low permeability layer is higher over the length of the model. Therefore, a reverse crossflow is observed where oil migrates from the low to the high permeability layer. The timing of the pressure differential reversal differs depending on the rock, oil and displacing water properties.

At an unfavourable modified mobility ratio, we do not see the typical crossflow of polymer solution and water from the high to the low permeability layer at the back of the slug and a balancing reciprocal flow of oil at the front of the slug from the low to the high permeability layer. This explains the negative crossflow values of oil coming out of the higher permeability layer seen in Figure 22 at all slug values simulated. Considering the results holistically for the cases with unfavourable mobility

ratios shows that the optimum slug size is at 0.75 PV as seen in Figure 23 which is higher than the reported value of 0.4 PV at a modified mobility ratio of 0.53 in secondary polymer floods.

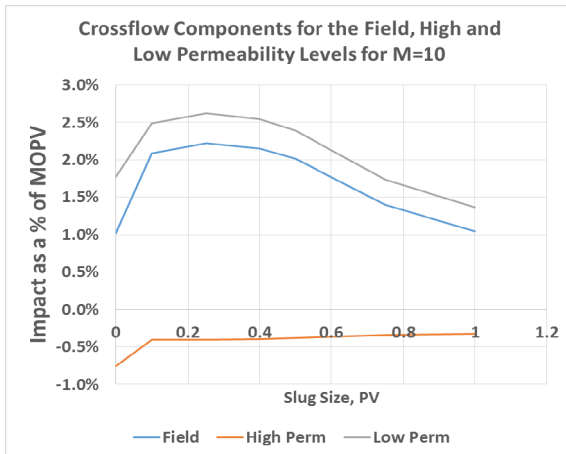


Figure 22 plot showing the crossflow components for secondary polymer floods of field, high and low permeability layer levels for $M=10$ vs. polymer slug size.

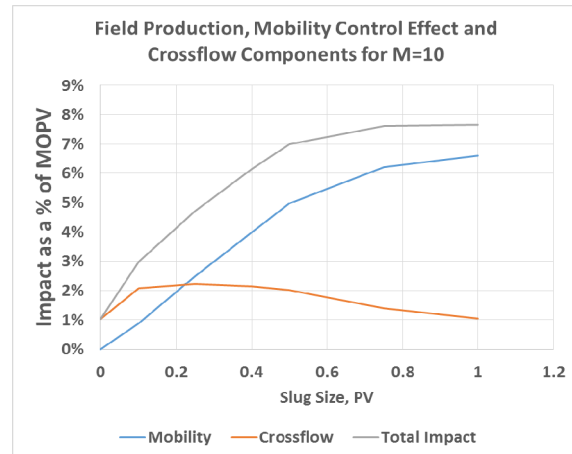


Figure 23 Plot showing a breakdown of total secondary polymer flooding impact to a viscous crossflow and mobility control components at $M=10$ vs. slug size.

In the case of tertiary polymer floods, we see the same trend with increasing slug size for viscous crossflow and mobility control when the value of modified mobility ratio is favourable, however, as with the results seen earlier, the additional recovered oil is less when compared with secondary polymer flood as evident in Figures 24 and 25. The optimum slug size for favourable tertiary polymer floods is 0.75 PV which is higher than the results seen in the secondary polymer flood cases of 0.4 PV.

On the other hand, when the modified mobility ratio is unfavourable, the crossflow impact on the field is negative indicating that the field is producing less oil compared to a similar case with no crossflow in the system. The trend has an upside, because as the slug size increases the retarded oil production is reduced. Combining the effects of crossflow and mobility control for this particular case shows that a tertiary polymer flood will only be successful in producing additional oil if the slug size is higher than 0.4 PV, with the highest gains observed at 1 PV as can be seen in Figures 26 and 27.

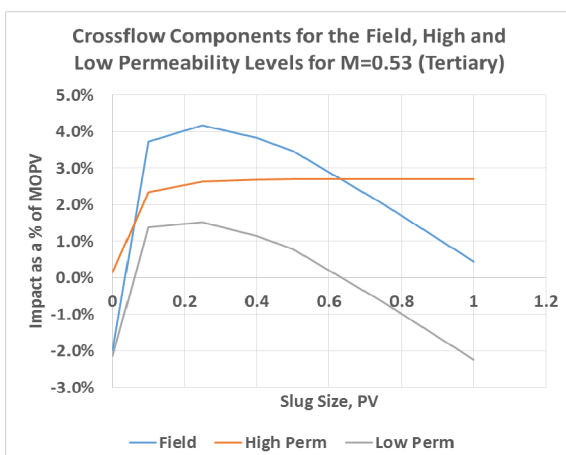


Figure 24 plot showing the crossflow components for tertiary polymer floods of field, high and low permeability layer levels for $M=0.53$ vs. polymer slug size.

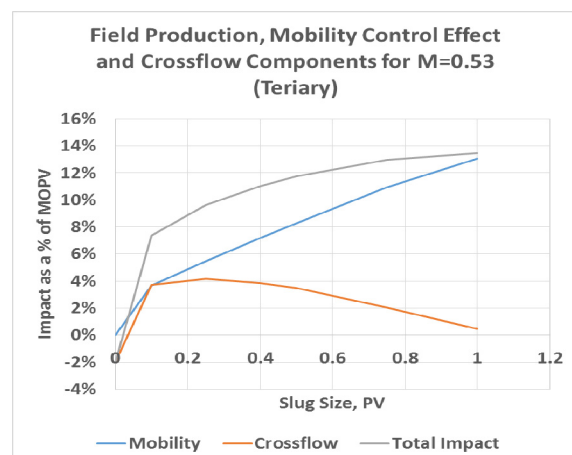


Figure 25 Plot showing a breakdown of total tertiary polymer flooding impact to a viscous crossflow and mobility control components at $M=0.53$ vs. slug size.

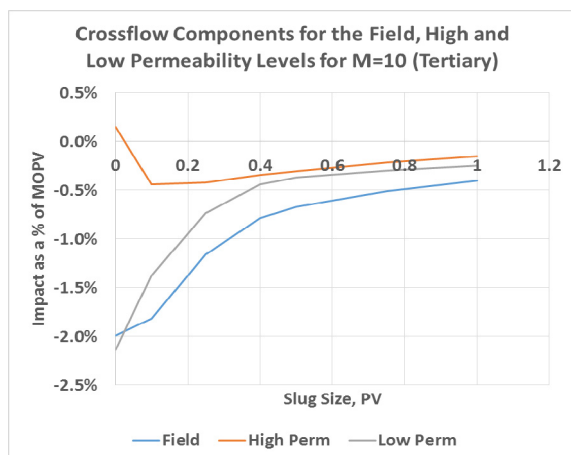


Figure 26 plot showing the crossflow components for tertiary polymer floods of field, high and low permeability layer levels for $M=10$ vs. polymer slug size.

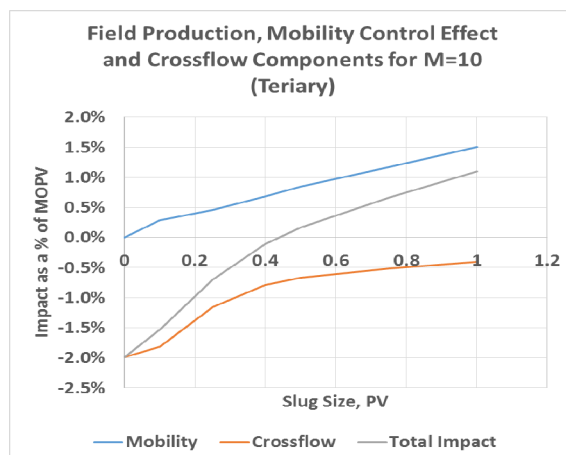


Figure 27 Plot showing a breakdown of total tertiary polymer flooding impact to a viscous crossflow and mobility control components at $M=10$ versus slug size.

Conclusions

The aim of this paper was to evaluate how rock and fluid properties impact the magnitude of viscous crossflow in a simple two-layered model in both secondary and tertiary polymer flooding modes.

We derived through inspectional analysis the 6 dimensionless numbers necessary to describe a polymer flood in a simple 2D two-layered model with constant pressure boundaries. The modified mobility ratio produced from the inspectional analysis incorporates the viscosities of oil, water and polymer solution interacting with each other in polymer floods. Including all of the fluid viscosities into one number reduces the need to have multiple mobility ratios to describe the oil/water, oil/polymer solution and water/polymer solution systems. Numerical simulations were performed for different scale size models but with the same dimensionless numbers. The results showed the validity of the numbers as both water cut and dimensionless production agreed for all different scale sizes.

We used ECLIPSE 100 to perform a numerical sensitivity analysis on both secondary and tertiary polymer floods with the following results:

- Maximum viscous crossflow was observed at moderate layer permeability ratios values and a favourable modified mobility ratio values.
- In this study, it was concluded that as the modified mobility ratio increases coupled with having layer permeability ratio values above 5 and 10 for secondary and tertiary polymer floods respectively, the amount of viscous crossflow decreases.
- Mobility control in polymer floods dominates the recovery in almost all cases tested.
- Viscous crossflow improves recovery and flood front conformance by accelerating the production of oil in the low permeability layer as well as cross flowing of oil to the high permeability layer
- Polymer flooding is most effective if initiated immediately rather than being performed post waterflood.
- Dilution of the slug size is observed as the slug moves through the high permeability layer due to viscous crossflow at the trailing edge of the slug.
- Maximum slug size reduction was observed at moderate layer permeability ratios and favourable modified mobility ratios, echoing the results seen in oil crossflow.
- The optimum slug size for secondary polymer floods was found to be 0.4 PV for favourable modified mobility ratios and 0.75 PV for unfavourable modified mobility ratios
- The optimum slug size for tertiary polymer floods was found to be at 0.75 PV for favourable modified mobility ratios and 1 PV for unfavourable modified mobility ratios

- Large slug sizes will not add more incremental oil and therefore might impact negatively on project economics.

Nomenclature

ϕ	Porosity	Fraction
k	Permeability	L^2
h	High permeability layer thickness	L
μ	Viscosity	m/(TL)
S	Saturation	Fraction
n	Corey Exponent	Dimensionless
k _{0r}	End Point Relative Permeability	Fraction
P	Pressure	m/(T ² L)
ρ	Phase density	m/L ³
IPV	Inaccessible Pore Volume IPV	Fraction
ω	Todd-Longstaff Mixing Parameter	Fraction
H	Model thickness	L
L	Model length	L
M	Modified mobility ratio	Dimensionless
m	Mass	m
T	Time	T

Subscripts

o	Oil
w	Water
p	Polymer solution
0	Initial
eff	Effective
a	High permeability layer
b	Low Permeability layer
max	maximum
or	Residual oil
wc	Connate water
c	Capillary
in	Inlet
out	Outlet

Acknowledgment

The author would like to thank Saudi Aramco for funding the research. Also, appreciation goes to Schlumberger for providing ECLIPSE to conduct the study.

References

Ahmed, G., Castanier, L. M. and Brigham, W. E. [1988] An experimental Study of Waterflooding From a Two-Dimensional Layered Sand Model. *SPE Reservoir Engineering, Society of Petroleum Engineers*, **3**, 45-54.

AlHamdan, M., Cinar, Y., Suicmez, V. S., and Dindoruk, B. [2011]. Experimental and Numerical Study of Compositional Two-Phase Displacements in Layered Porous Media. *SPE Reservoir Characterisation and Simulation Conference and Exhibition*, 9-11 October, Abu Dhabi, UAE. doi:10.2118/147967-MS

Cinar, Y., Jessen, K., Berenblyum, R., Juanes, R., and Orr, F. M. [2006]. An Experimental and Numerical Investigation of Crossflow Effects in Two-Phase Displacements. *SPE Journal, Society of Petroleum Engineers*, **11**, 216-226. doi:10.2118/90568-PA

Clifford, P. J. and Sorbie, K. S. [1985] The Effects of Chemical Degradation on Polymer Flooding. *SPE Oilfield and Geothermal Chemistry Symposium*. Phoenix, USA: Society of Petroleum Engineers.

Debbabi, Y., Jackson, M. D., Hampson, G. J., Fitch, P. J. R., and Salinas, P. [2016] The interplay of Capillary and Viscous Forces Driving Flow through Layered Porous Media. *15th Eropean Conference on the Mathematics of Oil Recovery* 29th August – 1st September, Amsterdam, Netherlands.

Lake, L. W. [1989] *Enhanced Oil Recovery*, Prentice Hall.

Pye, D. J. [1964] Improved secondary recovery by control of water mobility. *Journal of Petroleum Technology*, **16**, 911-916.

Sandiford, B. B. [1964] Laboratory and Field Studies of Water Floods Using Polymer Solutions to Increase Oil Recoveries. *Journal of Petroleum Technology*, **16**, 16.

Seright, R. S. [2016]. How Much Polymer Should Be Injected During a Polymer Flood? Review of Previous and Current Practices. *Society of Petroleum Engineers*. doi:10.2118/179543-PA

Shook, M., Li, D., Lake, L. W. [1992] Scaling Immisible Flow Through Permeable Media by Inspectional Analysis. *In-Situe*, **4**, 311-349.

Shotton, M., Stephen, K. and Giddins, M. [2016] High-Resolution Sudies of Polymer Flooding in Heterogeneous layered Reservoirs. *SPE EOR Conference at Oil and Gas West Asia*. Muscat, Oman, 21-23 March, 2016.

Sorbie, K. S. and Seright, R. S. [1992] Gel Placement in Heterogeneous Systems with Crossflow. *8th SPE/DOE Symposium on Enhanced Oil Recovery*. Tulsa, Oklahom, April 22-24, 1992.

Sorbie, K. S. [1991] *Polymer-Improved Oil Recovery*, Blackie.

Sorbie, K. S., Sheb, M., Hosseini, A. and Wat, R. M. S. [1990] Scaled Miscible Floods in Layered Beadpacks Investigating Viscous Crossflow, the Effects of Gravity, and the Dynamics of Viscous Slug Breakdown. *SPE Annual Technical Conference and Exhibition*. New Orleans: Society of Petroleum Engineers.

Sorbie, K. S. and Walker, D. J. [1988] A Study of the Mechanism of Oil Displacement Using Water and Polymer in Stratified Laboratory Core Systems. *SPE Enhanced Oil Recovery Symposium*. Tulsa, USA: Society of Petroleum Engineers.

Wright, R. J., Wheat, M. R., and Dawe, R. A. [1987]. Slug Size and Mobility Requirements for Chemically Enhanced Oil Recovery Within Heterogeneous Reservoirs. *SPE Reservoir Engineering, Society of Petroleum Engineers*, **2**, 92-102 doi:10.2118/13704-PA

Zapata, V. J. and Lake, L. W. [1981]. A Theoretical Analysis of Viscous Crossflow. *SPE Annual Technical Conference and Exhibition*, San Antonio, Texas, October 4-7 doi:10.2118/10111-MS